Hindawi
Analytical Cellular Pathology
Volume 2023, Article ID 1761398, 19 pages
https://doi.org/10.1155/2023/1761398

Research Article

Construction of a Cuproptosis-Related lncRNA Prognostic Model for Bladder Urothelial Carcinoma and Screening of Potential Drugs

Xuzhan Ma[1] **and Libin Sun**[2]

[1]*Department of Interventional Radiology, Affiliated Hospital of Shanxi University of Chinese Medicine, Taiyuan, Shanxi, China*
[2]*Department of Urology, Affiliated First Hospital of Shanxi Medical University, Taiyuan, Shanxi, China*

Correspondence should be addressed to Libin Sun; sunlibin1987@sina.com

Received 14 December 2022; Revised 17 April 2023; Accepted 24 April 2023; Published 25 May 2023

Academic Editor: Consuelo Amantini

Objective. This study aimed to analyze the cuproptosis-related long non-coding RNA (lncRNA) in patients with bladder urothelial carcinoma (BLCA), construct a prognostic model, and screen its potential drugs. *Methods*. The transcriptome expression and clinical and mutation burden data related to BLCA were downloaded from The Cancer Genome Atlas database. The prognostic lncRNAs were screened using univariate Cox and Lasso regression analyses, and then included in the multifactor risk ratio model. The risk score of each sample was calculated based on the prognostic model formula, and the patients were divided into high- and low-risk groups for survival difference analysis. Clinically relevant receiver operating characteristic (ROC) curve, *C*-index principal component analysis, and clinical data statistics were used to evaluate the predictive power of the model. The risk-differential lncRNAs were functionally enriched. We calculated the tumor mutation burden of risk lncRNAs, and survival and the Tumor Immune Dysfunction and Exclusion analyses for high- and low-risk groups. Finally, immunocorrelation analysis and potential drug screening were performed. *Results*. Eleven lncRNAs with independent prognostic significance were screened out to construct the prognostic model. Survival analysis showed a significant difference in survival between the high- and low-risk groups. The areas under the ROC curve at 1, 3, and 5 years were 0.711, 0.679, and 0.713, respectively. The discrimination between the lncRNA high- and low-risk groups in the constructed model was the most obvious. The risk-differential lncRNAs were closely related to immunity. The treatment drugs with high sensitivity were screened based on the IC50 value. *Conclusion*. The 11 cuproptosis-related lncRNAs may serve as molecular biomarkers and therapeutic targets for BLCA.

1. Introduction

Bladder cancer (BC) is a malignant tumor occurring on the bladder mucosa, among which transitional cell carcinoma is the most common one and is called bladder urothelial carcinoma (BLCA). BC is the most common malignant tumor of the urinary system in China and ranks 10th in the incidence of all types of cancer in the world [1, 2]. Despite medical developments, improved diagnostics, and increased health awareness in recent years, the incidence has not been stable throughout the world over time, nor will it be in the near future. Countermeasures should be taken to deal with the adverse effects of aging [3].

The main treatments of BC at present include surgery, radiotherapy, chemotherapy, immune support, and so on. Invasive BC accounts for about 70% of all BCs, and the muscle layer is generally involved in the resection of transurethral bladder tumor, but the possibility of recurrence and progression is higher. Muscularis invasive BC accounts for about 30% of all BCs, and radical resection and bladder pelvic lymph node cleaning treatment are the gold standard. However, still, a high recurrence rate or the possibility of

Table 1: Co-expression of cuproptosis-related genes and lncRNA of BLCA (partial examples).

Cuproptosis-related genes	lncRNAs	cor	P -value	Regulation
CDKN2A	CDKN2A-DT	0.80438382	9.43×10^{-95}	Positive
NLRP3	AC090559.1	0.68679608	8.91×10^{-59}	Positive
DBT	AC108052.1	0.67085575	3.42×10^{-55}	Positive
DBT	LIMD1-AS1	0.65036636	6.69×10^{-51}	Positive
DBT	LINC02109	0.62524963	4.50×10^{-46}	Positive
DBT	AC006017.1	0.61358812	5.60×10^{-44}	Positive
DBT	AC018616.1	0.61068595	1.80×10^{-43}	Positive
DBT	C21orf62-AS1	0.61056131	1.90×10^{-43}	Positive
DBT	AC022150.4	0.60747919	6.48×10^{-43}	Positive
DBT	AC099482.1	0.60103282	8.10×10^{-42}	Positive

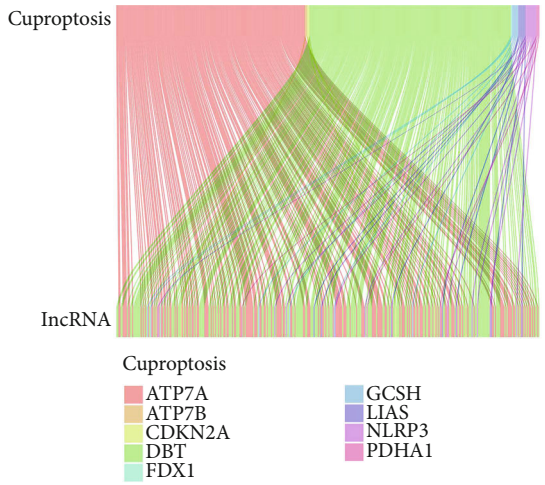

Figure 1: The correlation between cuproptosis-related genes and lncRNA.

progression exists [4, 5]. Currently, authoritative guidelines recommend immune checkpoint inhibitors as the second-line treatment in patients with BC who have developed metastases and lost the chance of surgical resection, and as the first-line treatment in patients with programmed death-ligand 1 (PD-L1) who are ineligible for platinum-based chemotherapy [6].

A variety of prespecified and precisely controlled programmed cell death occur, such as apoptosis, necroptosis, pyroptosis, and ferroptosis, during the development of multicellular organisms. The mechanism of copper toxicity has been demonstrated to be different from all other known mechanisms regulating cell death, and this previously uncharacterized cell death mechanism is termed cuproptosis [7].

Therefore, this study used The Cancer Genome Atlas (TCGA) database to predict the long non-coding RNA (lncRNA) associated with copper mortality in BC, so as to construct the prognostic model of related lncRNA and screen potential drugs in patients with BLCA.

2. Materials and Methods

2.1. Data Downloading and Sample Sorting. The BLCA-related transcriptome expression data, clinical data, and the mutation load were downloaded from the National Cancer Institute GDC Data Portal website (https://portal.gdc.cancer.gov), which included the control and the patient's clinical data, such as age, sex, survival time and survival state, tumor classification, T stage, N stage, and M installment. The Perl software was used to collate the transcriptome data and transformation ID, and separate lncRNA and microRNA.

2.2. Expression of Cuproptosis-Related lncRNA and Co-Expression Analysis. The limma package of the R-Studio software was used to collate transcriptome data and perform cuproptosis-related gene (*NFE2L2*, *NLRP3*, *ATP7B*, *ATP7A*, *SLC31A1*, *FDX1*, *LIAS*, *LIPT1*, *LIPT2*, *DLD*, *DLAT*, *PDHA1*, *PDHB*, *MTF1*, *NFE2L2*, *NLRP3*, *ATP7B*, *ATP7A*, *SLC31A1*, *FDX1*, *LIAS*, *LIPT1*, *LIPT2*, *DLD*, *DLAT*, *PDHA1*, *PDHB*, *MTF1*, *GLS*, *CDKN2A*, *DBT*, and *GCSH DLST*) analysis. The extraction of the lncRNA expression quantity associated with cuproptosis via the limma package quantity of cuproptosis-related gene expression was analyzed via lncRNA isolation (set conditions: corFilter = 0.4 and $P < 0.001$).

2.3. Construction of the Prognostic Model. The limma package of the R-Studio software was used to merge cuproptosis-related lncRNA expression data with the clinical data (survival time and survival state) via the survival pack, the caret bag, glmnet package, survminer merged data and time receiver operating characteristic (ROC) package, and univariate Cox regression analysis (filter criteria: $P < 0.05$) to screen the lncRNA related to the prognosis in patients with BLCA. Further screening analysis was performed by Lasso regression to reduce overfitting of the data and to screen the key cuproptosis-related lncRNAs. Cross-validation was used in Lasso regression to select parameters, and the Lasso regression coefficient spectrum was drawn. Finally, multivariate Cox regression analysis was performed to establish a valuable lncRNA model for the

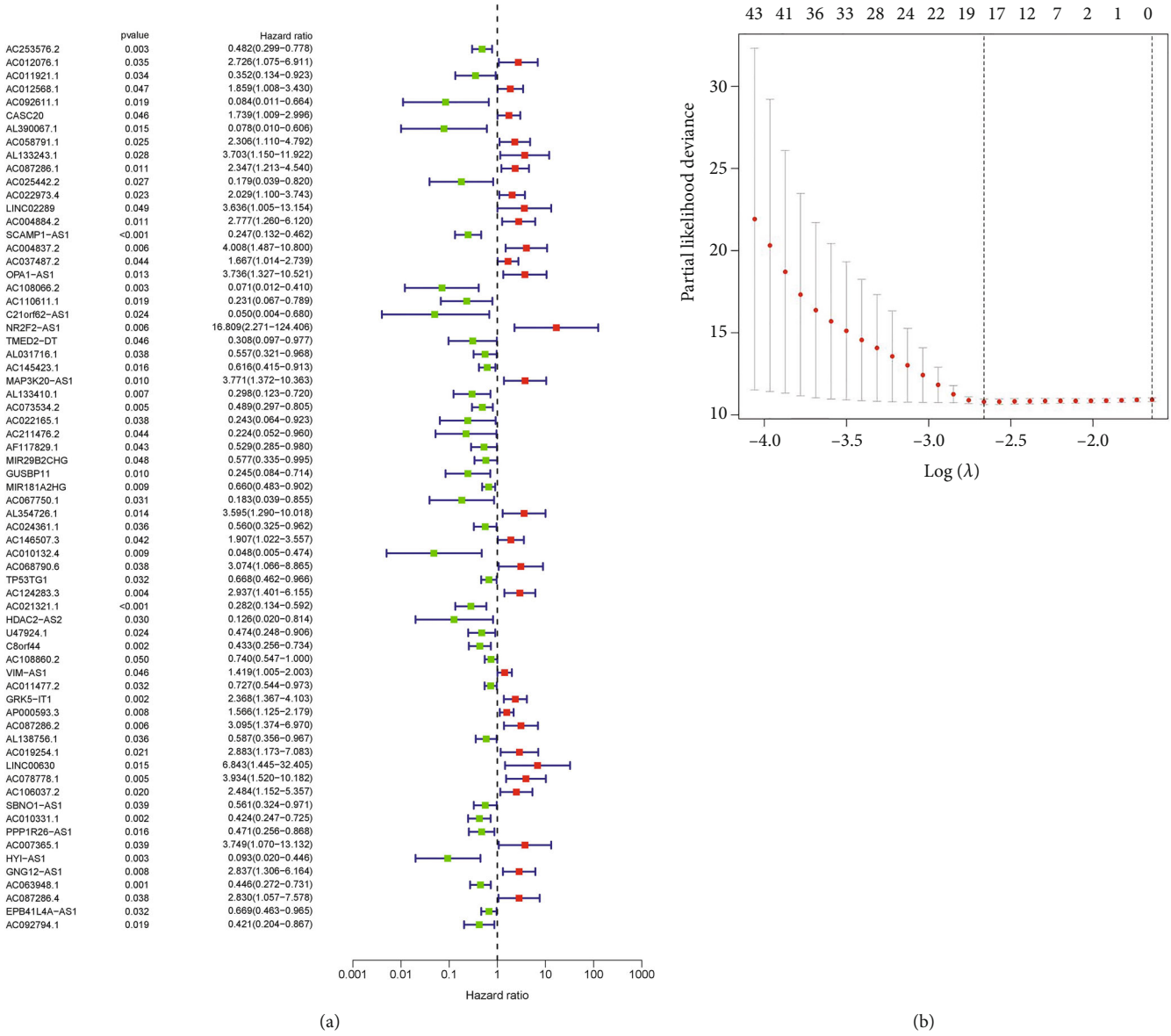

Figure 2: Continued.

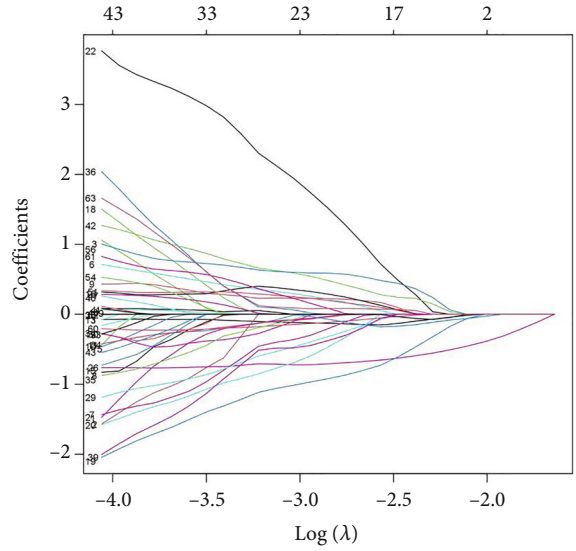

(c)

Figure 2: Screening for cuproptosis-related lncRNA of greater prognostic value in patients with BLCA. (a) Univariate Cox analysis of lncRNA associated with cuproptosis. (b) and (c) Lasso regression analysis of lncRNA associated with cuproptosis.

Table 2: Multivariate Cox analysis of lncRNA associated with cuproptosis.

ID	Coefficient
CASC20	0.686828262
'SCAMP1-AS1'	−0.910543962
AC108066.2	−1.920725726
AC110611.1	−2.506788801
'NR2F2-AS1'	3.872755402
AC022165.1	−1.145970684
MIR181A2HG	−0.342648292
AC010132.4	−1.908268477
AC124283.3	1.504962992
AP000593.3	0.340927746
AC078778.1	1.373238179

prognosis of BLCA and presented in the form of a nomogram. The lncRNA model was constructed based on the multivariate Cox regression analysis, and the risk score equation was: Risk score = $\sum_{i=1}^{n}$coefficient(i) × EXP(lncRNA)i. The data were randomly divided into two groups: Train group and Test group.

2.4. Evaluation and Clinical Value Analysis of the Prognostic Model. The R-Studio software was used to perform clinical statistical analysis between the Train and Test groups. Limma, reshape2, tidyverse, and ggplot2 packages were used for correlation analysis of cuproptosis-related gene expression data, cuproptosis-related lncRNA expression data, and risk gene data. The survival, survMiner, and timeROC packages were used to analyze the OS and progression-free survival (PFS) of risk gene data. Independent prognostic and ROC analyses were performed on risk gene and clinical data. The *C*-index analysis was performed using dplyr, survival, rms, and pec packages. Risk genetic data and clinical data were analyzed by using regplot, survival and rms packages, and then histogram was drawn to predict the survival of BLCA patients by nomogram. Survival was analyzed using the R-Studio software package and survminer package data for risk genes associated with clinical data, and the validation model built was applicable to patients with different clinical groups. The principal component analysis (PCA) was performed using the limma and Scatterplot3d packages to verify whether the lncRNA involved in the model could distinguish the patients in the high- and low-risk groups.

2.5. Screening of Risk Genes with Significant Differences and Enrichment and Immune-Related Functional Analyses. The R-Studio software was used to conduct risk difference analysis on risk gene data and gene expression data, and to screen the differential risk genes with significant differences. The Gene Ontology (GO) and Kyoto Encyclopedia of Genes and Genomes (KEGG) enrichment analyses were performed. Then, risk gene data and gene expression data were analyzed for immune-related functions, and statistically significant differences in immune-related functions were observed between the high- and low-risk groups.

2.6. Comparison between High and Low Risk of BC Risk Gene Mutation Frequency and Mutation Load Survival Analysis. The downloaded mutation burden data were processed using the Perl software, and the mutation burden of BLCA was calculated. The Perl software was used to process the tumor mutation data and risk gene data to obtain the mutation gene data of high- and low-risk groups. The MafTools package of the R-Studio software was used to analyze the mutation frequency of risk genes between high- and low-

Table 3: Clinical statistical analysis of groups.

Covariates	Type	Total	Test	Train	*P*-value
Age (years)	≤65	159 (39.36%)	75 (37.13%)	84 (41.58%)	0.4152
	>65	245 (60.64%)	127 (62.87%)	118 (58.42%)	
Gender	Female	106 (26.24%)	49 (24.26%)	57 (28.22%)	0.4286
	Male	298 (73.76%)	153 (75.74%)	145 (71.78%)	
Grades	High grade	381 (94.31%)	193 (95.54%)	188 (93.07%)	0.4841
	Low grade	20 (4.95%)	8 (3.96%)	12 (5.94%)	
	Unknown	3 (0.74%)	1 (0.5%)	2 (0.99%)	
Stages	Stage I	2 (0.5%)	2 (0.99%)	0 (0%)	0.4932
	Stage II	128 (31.68%)	61 (30.2%)	67 (33.17%)	
	Stage III	140 (34.65%)	70 (34.65%)	70 (34.65%)	
	Stage IV	132 (32.67%)	68 (33.66%)	64 (31.68%)	
	Unknown	2 (0.5%)	1 (0.5%)	1 (0.5%)	
T	T0	1 (0.25%)	1 (0.5%)	0 (0%)	0.8389
	T1	3 (0.74%)	2 (0.99%)	1 (0.5%)	
	T2	117 (28.96%)	57 (28.22%)	60 (29.7%)	
	T3	193 (47.77%)	97 (48.02%)	96 (47.52%)	
	T4	57 (14.11%)	29 (14.36%)	28 (13.86%)	
	Unknown	33 (8.17%)	16 (7.92%)	17 (8.42%)	
M	M0	194 (48.02%)	98 (48.51%)	96 (47.52%)	1
	M1	11 (2.72%)	6 (2.97%)	5 (2.48%)	
	Unknown	199 (49.26%)	98 (48.51%)	101 (50%)	
N	N0	235 (58.17%)	115 (56.93%)	120 (59.41%)	0.926
	N1	46 (11.39%)	25 (12.38%)	21 (10.4%)	
	N2	75 (18.56%)	38 (18.81%)	37 (18.32%)	
	N3	6 (1.49%)	3 (1.49%)	3 (1.49%)	
	Unknown	42 (10.4%)	21 (10.4%)	21 (10.4%)	

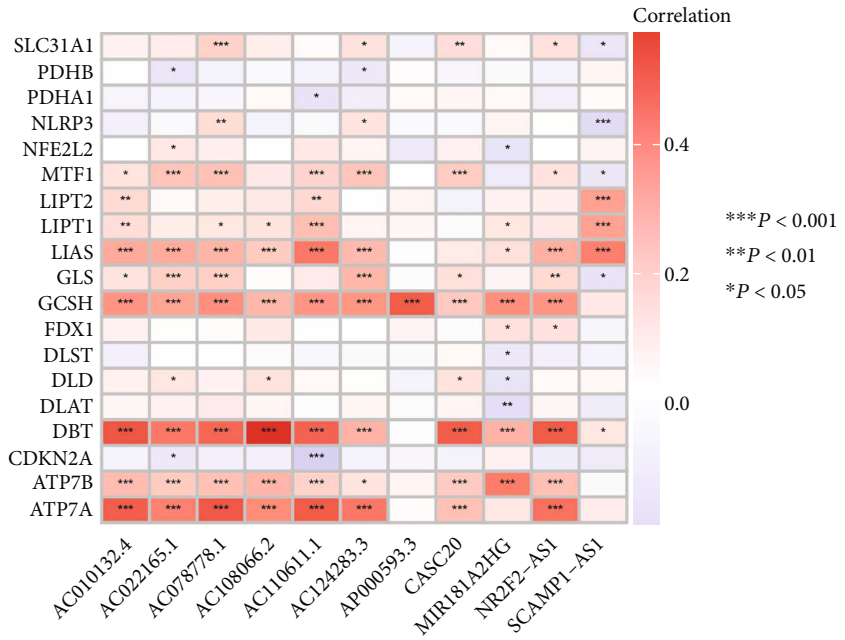

Figure 3: Correlation between lncRNA involved in model construction and cuproptosis-related genes.

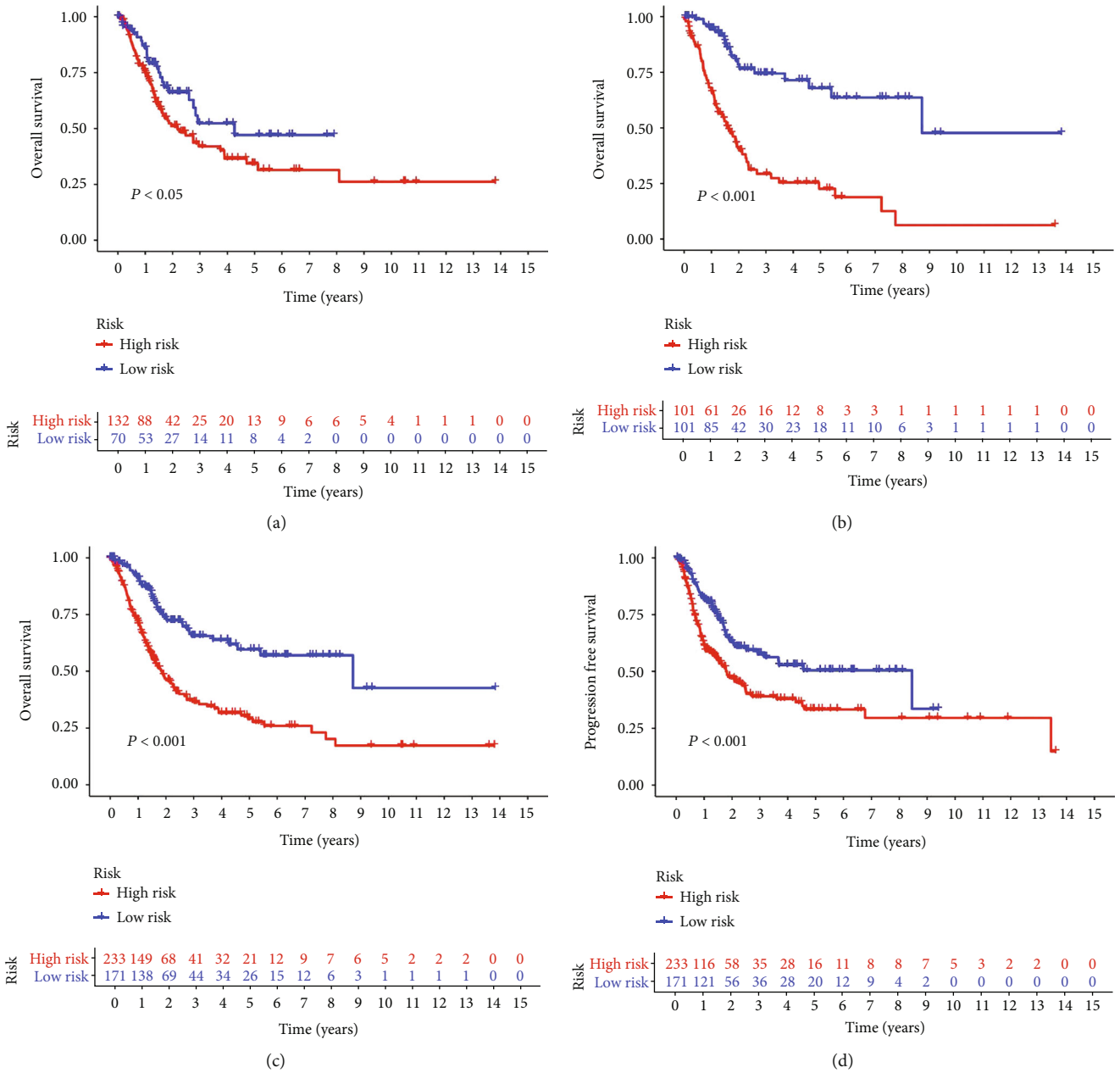

Figure 4: OS and PFS analyses between high- and low- risk groups in Train group and Test group. (a) OS analysis of all risk lncRNAs with high and low risk. (b) OS analysis of train group with high and low risk. (c) OS analysis of test group with high and low risk. (d) PFS analysis of all risk lncRNAs with high and low risk.

risk groups. Reuse the survival of cancer mutations and the survminer package load data and risk genes in the tumor mutation load of survival analysis.

2.7. Analysis of Immune Evasion and Immunotherapy in BLCA. The transcriptome data were uploaded to the Tumor Immune Dysfunction and Exclusion (TIDE) database (http://tide.dfci.harvard.edu/) to obtain the TIDE rating of the transcriptome data. The R-Studio software limma package and ggpubr package were used to analyze risk genes data. The high- and low-TIDE scores were analyzed to find the difference between the risk groups.

2.8. BC Screening of Potential Drugs. Gene expression data and risk genes were analyzed using the limma, ggpubr, pRRophetic bags, and ggplot2 packages, and screening indicated a significant difference between high- and low-risk groups of drugs (filter condition: $P < 0.001$).

3. Results

3.1. Extraction of Cuproptosis-Related lncRNA Expression and Co-Expression Analysis. Using the Perl transcriptome data processing software, we obtained 16,876 lncRNAs from the data set of RNA-seq of 412 samples of BLCA

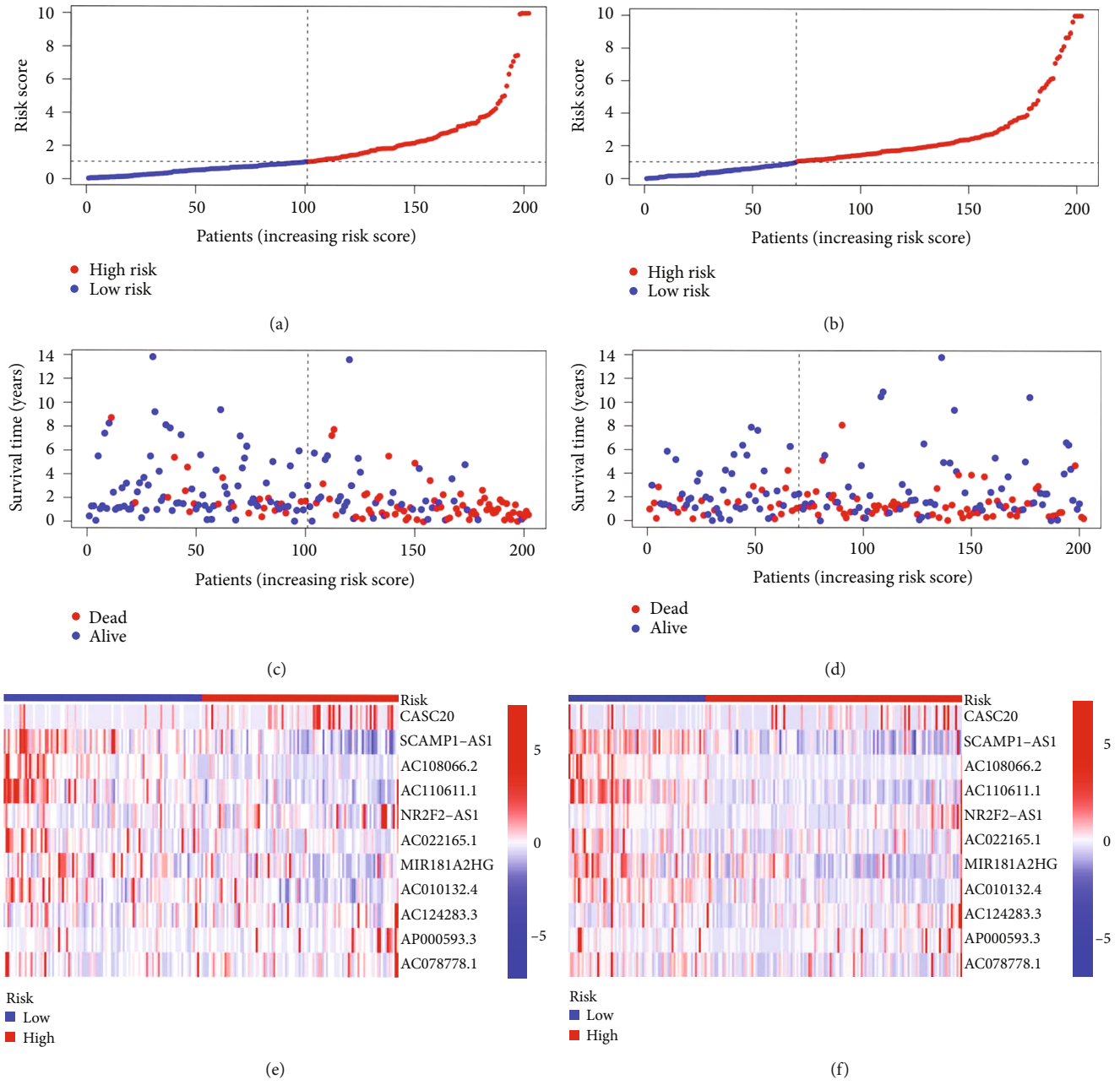

Figure 5: Patient risk score in relation to risk and survival and the expression analysis of 11 screened lncRNA in the high and low risk of Train group and Test group. (a) Patient risk score was associated with risk in the Train group. (b) Patient risk score was associated with risk in the Test group. (c) Patient risk score was associated with survival in the Train group. (d) Patient risk score was associated with survival in the Test group. (e) Expression of 11 lncRNA screened in Train group in high- and low-risk groups. (f) Expression of 11 lncRNA screened in Test group in high- and low-risk groups.

and 19 corresponding tissue adjacent to carcinoma samples after isolating lncRNA expression data. The R-Studio software was used to analyze the transcriptome data of cuproptosis-related genes (*NFE2L2*, *NLRP3*, *ATP7B*, *ATP7A*, *SLC31A1*, *FDX1*, *LIAS*, *LIPT1*, *LIPT2*, *DLD*, *DLAT*, *PDHA1*, *PDHB*, *MTF1*, *GLS*, *CDKN2A*, *NFE2L2*, *NLRP3*, *ATP7B*, *ATP7A*, *SLC31A1*, *FDX1*, *LIAS*, *LIPT1*, *LIPT2*, *DLD*, *DLAT*, *PDHA1*, *PDHB*, *MTF1*, *GLS*, *CDKN2A*, *DBT*, and *GCSH DLST*). The expression levels of cuproptosis-related genes in each sample were obtained through analysis, and then combined with the obtained 16,876 lncrnas for co-expression analysis, a total of 762 copper-death co-expression lncrnas were screened (corFilter = 0.4, $P < 0.001$; Table 1). The R-Studio software was used to draw the mulberry map of the co-expression data, and the correlation between cuproptosis-related genes and lncRNA could be intuitively observed (Figure 1).

3.2. Construction of Prognostic Model. The R-Studio software was used to merge the lncRNA expression files related to

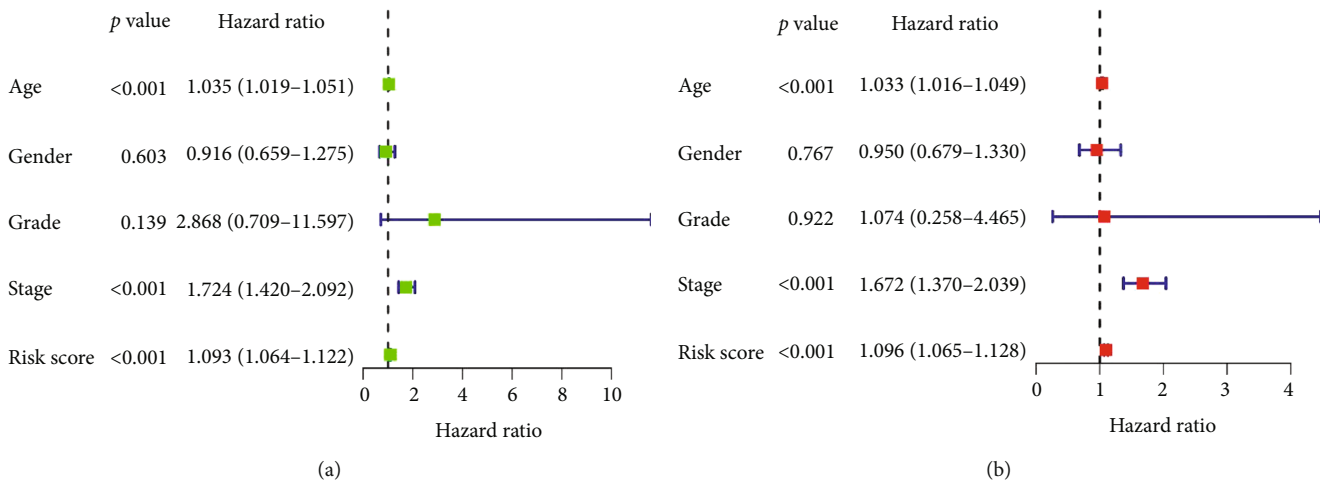

Figure 6: Independent prognostic analysis of the constructed model. (a) Univariate Cox analysis. (b) Multivariate Cox analysis.

cuproptosis with clinical data (survival time and survival status). Furthermore, 67 lncRNAs related to the prognosis of patients with BLCA were initially screened using univariate Cox regression analysis ($P < 0.05$; Figure 2(a)), and then, Lasso regression analysis was used to reduce the overfitting of data. Seventeen cuproptosis-related lncRNAs that were more valuable for the prognosis of patients with BLCA were screened (Figures 2(b) and 2(c)). Finally, 11 lncRNAs with prognostic values for copper mortality were screened out via multivariate Cox regression analysis (Table 2), and the prognostic model was constructed based on the risk scores of the screened-out 11 lncRNAs. The samples were randomly divided into two groups (Train and Test groups). The samples in the Train and Test groups were divided into high- and low-risk groups. The risk score was obtained using the following formula:

$$\begin{aligned}
&(0.686828262125213 \times \mathrm{CASC20}) \\
&+ (-0.910543962195588 \times \text{'SCAMP1} - \mathrm{AS1'}) \\
&+ (-1.92072572614444 \times \mathrm{AC108066.2}) \\
&+ (-2.5067888012423 \times \mathrm{AC110611.1}) \\
&+ \left(3.87275540196912 \times {}'\mathrm{NR2F2} - \mathrm{AS1'}\right) \\
&+ (-1.14597068371537 \times \mathrm{AC022165.1}) \\
&+ (-0.342648292263448 \times \mathrm{MIR181A2HG}) \\
&+ (-1.90826847655345 \times \mathrm{AC010132.4}) \\
&+ (1.50496299163889 \times \mathrm{AC124283.3}) \\
&+ (0.340927745829933 \times \mathrm{AP000593.3}) \\
&+ (1.37323817887309 \times \mathrm{AC078778.1}). \qquad (1)
\end{aligned}$$

3.3. Evaluation and Clinical Value Analyses of the Prognostic Model. Combined with the clinical data of patients with ccRCC, R-Studio software was used to conduct clinical statistical analysis of the training group and the Test group. No significant difference was observed in each clinical trait between the Train and Test groups, indicating no deviation in clinical traits between the random grouping of the samples ($P > 0.05$; Table 3). Correlation analysis was performed on the expression data of cuproptosis-related genes, cuproptosis-related lncRNA expression data, and risk gene data to know the correlation between lncRNA involved in the model construction and cuproptosis-related genes (Figure 3). The OS analysis of the risk gene data indicated significant differences in the survival rate between the high- and low-risk groups in the risk gene data, in both the Train and Test groups, and the survival of patients in the high-risk group in the risk gene data was shorter in both the Train and Test groups compared with those in the low-risk group. The PFS analysis of risk gene data showed a significant difference in the progression-free survival between the high- and low-risk groups, and the high-risk group had significantly shorter progression-free survival than the low-risk group (Figure 4). The R-Studio software was used to Train set and Test set the risk of genetic data is analyzed, through the risk curve can be intuitive grouping situation of both high- and low-risk groups (median of risk score), through the survival state diagram can be found that patients with increased risk, the cases of death also along with the increase, and by heat maps can be observed, CASC20, NR2F2-AS1, AC124283.3, AP000593.3 are high-risk lncRNA, secretory carrier membrane protein 1 (SCAMP1)-AS1, AC108066.2, AC110611.1, AC022165.1, MIR181A2HG, AC010132.4, and AC078778.1 were low-risk lncRNAs (Figure 5). Univariate and multivariate Cox regression analyses, via independent prognostic analysis of risk gene data and clinical relevant data (sex, age, grade, and stage), indicated that the constructed model could be used as an independent prognostic factor in patients with BLCA independent of other clinical traits (risk score $P < 0.001$; Figure 6). Combining the ROC curve with clinical relevant data revealed that the constructed model predicted the survival time of patients Area Under Curve (AUC) = 0.711) better than age, sex, grade, and stage. The ROC curve showed that the constructed model predicted the survival time in patients with BLCA with high sensitivity and accuracy (AUC after 1, 3, and 5 years was 0.711, 0.679, and 0.713, respectively). Furthermore, the *C*-index

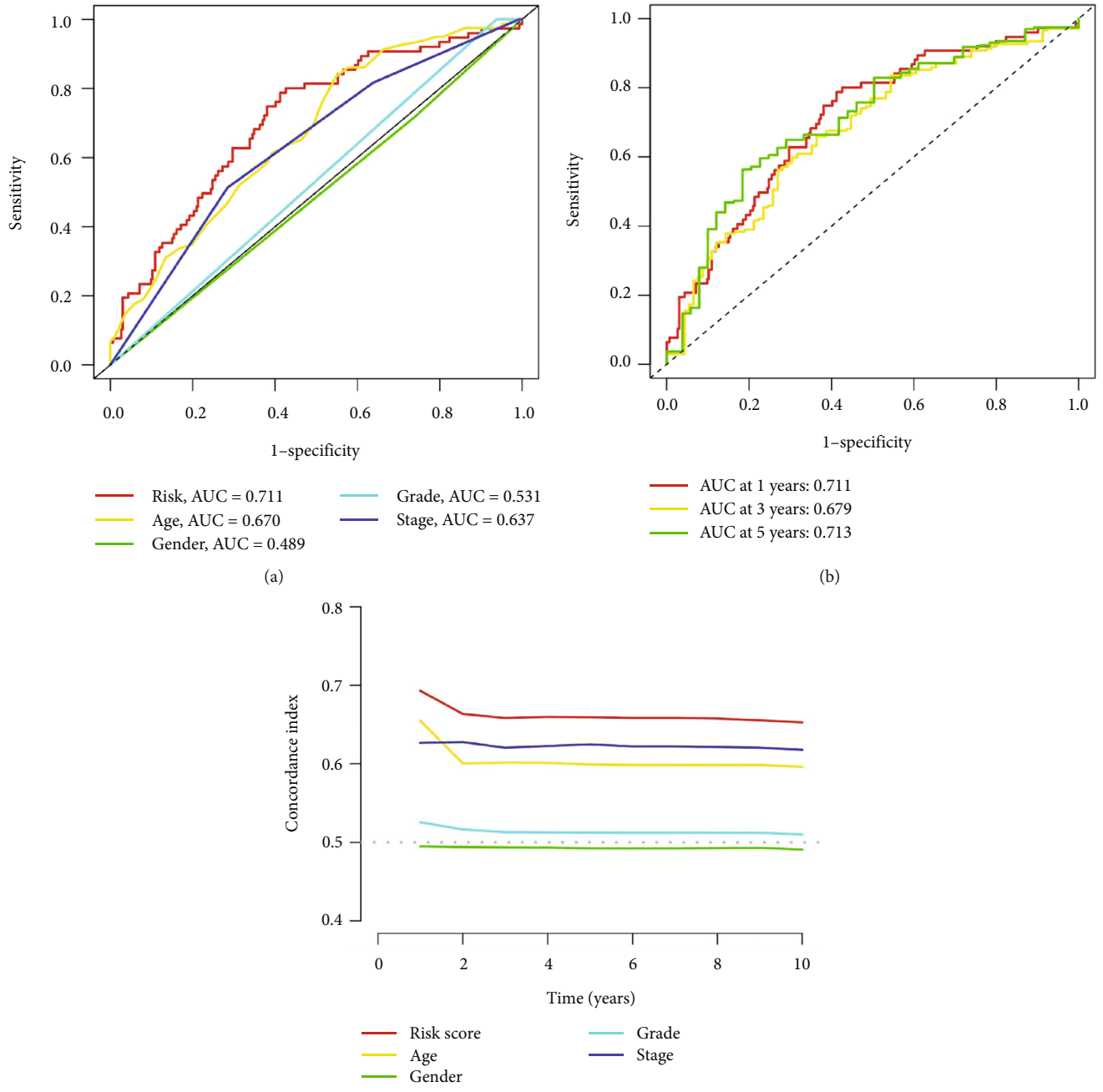

Figure 7: Continued.

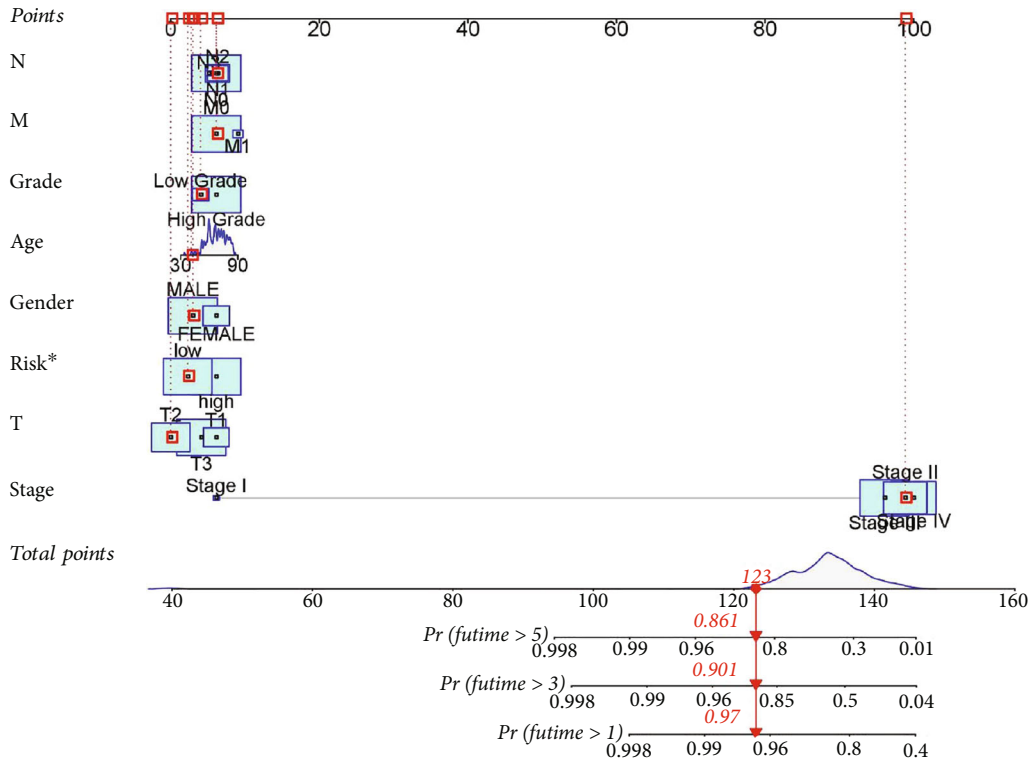

(d)

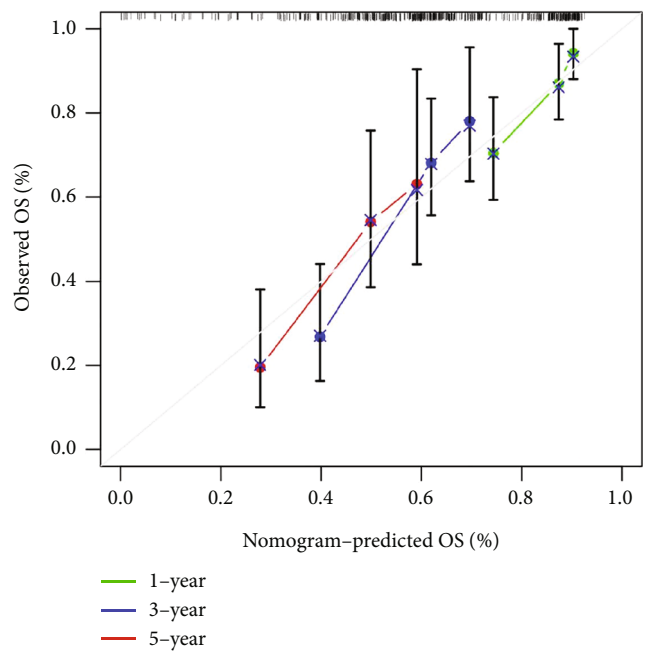

(e)

Figure 7: Analysis of the model to predict patient survival. (a) ROC curve of the constructed model. (b) The ROC curve of the constructed model was analyzed jointly with clinical data. (c) The *C*-index curve of the constructed model. (d) The survival column chart of patients with BLCA. (e) The calibration diagram of patients with BLCA.

curve showed that the model constructed had a high accuracy in predicting the survival of patients (Figures 7(a), 7(b), and 7(c)). The survival nomogram of patients with BLCA was drawn by combining the risk gene data with clinical relevant data, and the risk of patients could be scored by the nomogram to predict the survival rate after 1, 3, and 5 years. The calibration chart showed that the predicted probability was basically consistent with the actual probability (Figures 7(d) and 7(e)). The analysis of risk gene data and clinical relevant data (stages) revealed that

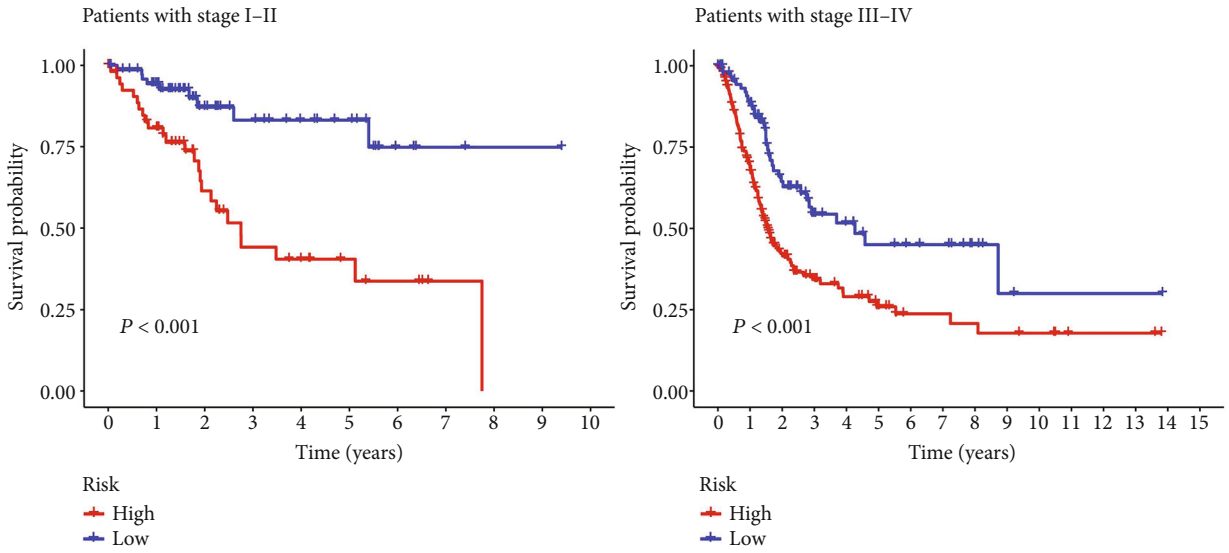

Figure 8: Analysis of risk gene data and clinically relevant data (Stages I and II and stages III and IV).

the constructed model was suitable for survival prediction in both Stages I and II and Stages III and IV patients ($P < 0.001$; Figure 8). PCA showed that the discrimination level between the lncRNA high- and low-risk groups in the constructed model was the most obvious, indicating that the patients in the high- and low-risk groups could be distinguished by the lncRNA involved in the model construction (Figure 9).

These results indicated that the prediction model based on 11 lncRNAs associated with copper mortality was significantly better than the clinical factors, such as age, sex, grade, and tumor stage, in predicting the prognosis of patients, and the risk score was significantly correlated with the progression of BLCA.

3.4. Screening and Enrichment Analysis of Risk Genes with Significant Differences. The R-Studio software was used for the differential analysis of gene expression data and risk gene data, and a total of 1042 genes with significant differences between the high- and low-risk groups were obtained (Table 4). The GO and KEGG enrichment analyses were further performed on the differential risk genes to analyze the enrichment pathways of differential risk genes in tumor tissues. The GO enrichment analysis showed that in the biological process of GO, differential risk genes were enriched in humoral immune response, extracellular matrix organization, extracellular structure organization, defense response to bacterium, phagocytosis, humoral immune response mediated by circulating immunoglobulin, complement activation classical pathway, collagen-containing extracellular matrix, immunoglobulin complex, circulating immunoglobulin complex, antigen binding, glycosaminoglycan binding, extracellular matrix structural constituent, immunoglobulin receptor binding, sulfur compound binding, cytokine receptor binding, cytokine activity, chemokine activity, and so on. The differential risk genes were enriched on GO:0003823, GO:0005539, GO:0005201, GO:0006959, GO:0045229, GO:0030198, GO:0043062, GO:0042742, GO:0006909, GO:0062023, and GO:0045229. The enrichment on GO:0019814 and GO:0009897 was significant (Figure 10(a)). The KEGG enrichment analysis showed that differential risk genes were enriched in cytokine–cytokine receptor interaction, viral protein interaction with cytokine and cytokine receptor, interleukin (IL)-17 signaling pathway, osteoclast differentiation, extracellular matrix–receptor interaction, protein digestion and absorption, phosphoinositide 3-kinase–Akt signaling pathway, chemokine signaling pathway, cell adhesion molecules, necrosis factor–kappa B signaling pathway, focal adhesion, proteoglycans in cancer, tumor necrosis factor signaling pathway, AGE–RAGE signaling pathway in diabetic complications, Janus kinase–signal transducer and activator of transcription signaling pathway, and transcriptional misregulation in cancer. The significant enrichment was observed on HSA05150, HSA04060, HSA04061, HSA05323, HSA05146, HSA04145, and HSA04640 (Figure 10(b)).

The immune-related function analysis of risk gene data and tumor gene expression data showed APC_co_inhibition, T_cell_co-inhibition, checkpoint, T_cell_co-stimulation, cytolytic_activity, inflammation promotion, Human Leukocyte Antigen (HLA), APC_co_stimulation, Chemokine receptors (CCR), Major Histocompatibility Complex (MHC)_class_I, and parainflammation. Significant differences were observed in Type_I_IFN_Reponse between the high- and low-risk groups ($P < 0.001$). Meanwhile, the heat map showed that the aforementioned immune-related functions were more active in the high-risk group (Figure 11).

3.5. Survival Analysis to Compare the Mutation Frequency and Mutation Burden of Risk Genes between High- and Low-Risk Groups of BLCA. The downloaded mutation burden data were processed using the Perl software, and the mutation burden of BLCA was calculated (Table 5). Risk genes for high- and low-risk groups of data of mutated genes, using the R-Studio software analysis between high- and low-risk group risk gene mutation frequency, and draw

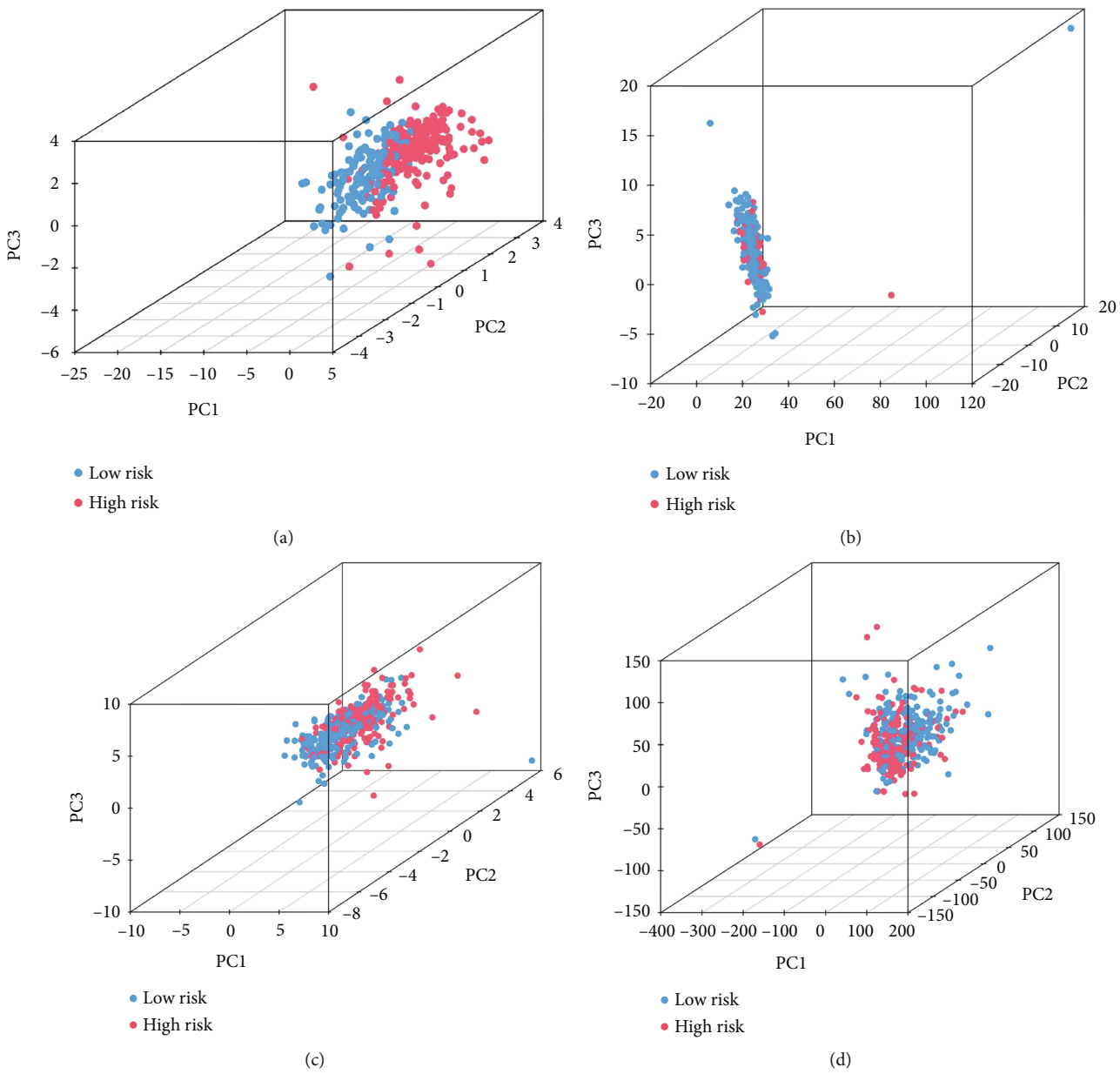

Figure 9: (a) PCA analysis of risk expression lncRNA. (b) Cuproptosis-related lncRNA. (c) Cuproptosis genes. (d) All genes.

a waterfall figure, can be found through the Perl software for tumor mutation data and data processing. The mutation frequency of risk genes in the high-risk group was mostly higher than that in the low-risk group (Figure 12(a)). Survival analysis of tumor mutation load data and risk genes showed that there was a significant difference in the survival time of patients with high and low mutation load, and the survival time of the group with high BLCA mutation load was longer than that of the group with low mutation load ($P < 0.001$; Figure 12(b)), high mutation load groups of high- and low-risk patients survival time has significant differences. The survival time of high-risk patients was shorter than that of low-risk patients ($P < 0.001$). A significant difference was observed in the survival time between high- and low-risk patients in the low-mutation burden group, with high-risk patients having a shorter survival time than low-risk patients ($P < 0.001$; Figure 12(c)).

3.6. Analysis of Immune Evasion and Immunotherapy in BLCA. The analysis of immune escape and immunotherapy of risk gene data indicated significant differences in TIDE scores between the high- and low-risk groups, and the TIDE scores in the high-risk group were significantly higher than that in the low-risk group, indicating that the immune escape potential in patients with BLCA in the high-risk group was greater, and hence, the effect of immunotherapy was worse ($P < 0.001$; Figure 13).

3.7. Screening of Potential Drugs for BLCA. The gene expression data and risk data for potential drug screening were

Table 4: Screening of differential risk genes (partial examples).

Gene	Low mean	High mean	logFC	*P*-value	fdr
FER1L4	47.19381988	12.700754	−1.8936837	1.08×10^{-28}	5.53×10^{-25}
AL390719.2	14.74714035	4.6966788	−1.6507224	1.31×10^{-28}	5.53×10^{-25}
AL450384.2	3.348402729	0.8479688	−1.9813899	2.13×10^{-28}	6.74×10^{-25}
RAD51-AS1	3.905567836	1.8979207	−1.0411126	3.79×10^{-28}	8.92×10^{-25}
ZNF436-AS1	2.065382456	0.8775648	−1.2348314	4.23×10^{-28}	8.92×10^{-25}
SH3BP5-AS1	1.707411696	0.7326129	−1.2206880	7.79×10^{-28}	1.41×10^{-24}
LINC02604	5.898293762	2.7048577	−1.1247450	1.88×10^{-27}	2.97×10^{-24}
AP002026.1	1.794942885	0.5660923	−1.6648288	3.29×10^{-27}	4.62×10^{-24}
PPFIBP2	14.22930877	5.1865937	−1.4560063	7.40×10^{-27}	8.95×10^{-24}
LINC00930	3.642230604	0.6977504	−2.3840394	7.79×10^{-27}	8.95×10^{-24}

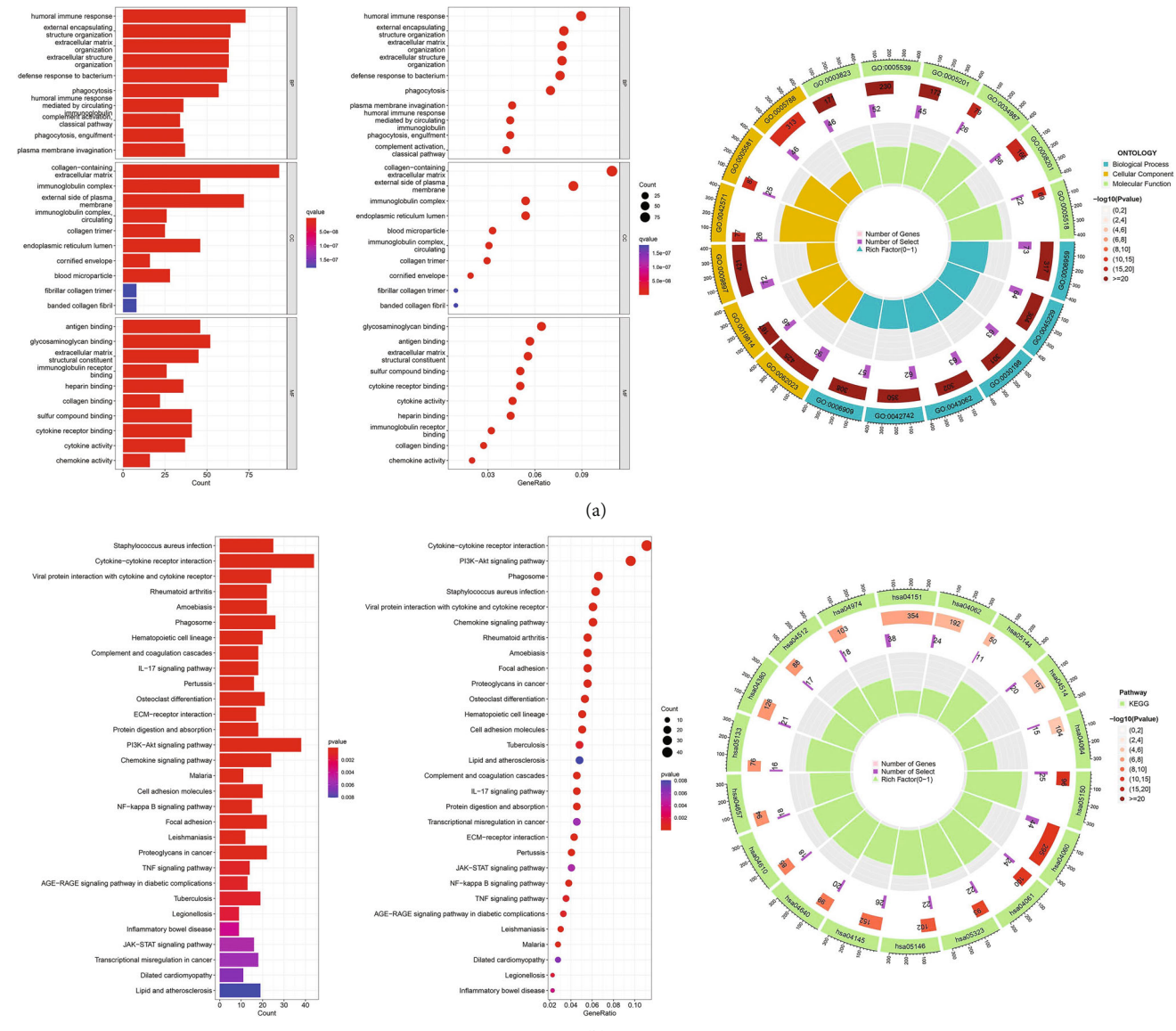

Figure 10: GO and KEGG enrichment analyses of differential risk genes. (a) GO enrichment analysis. (b) KEGG enrichment analysis.

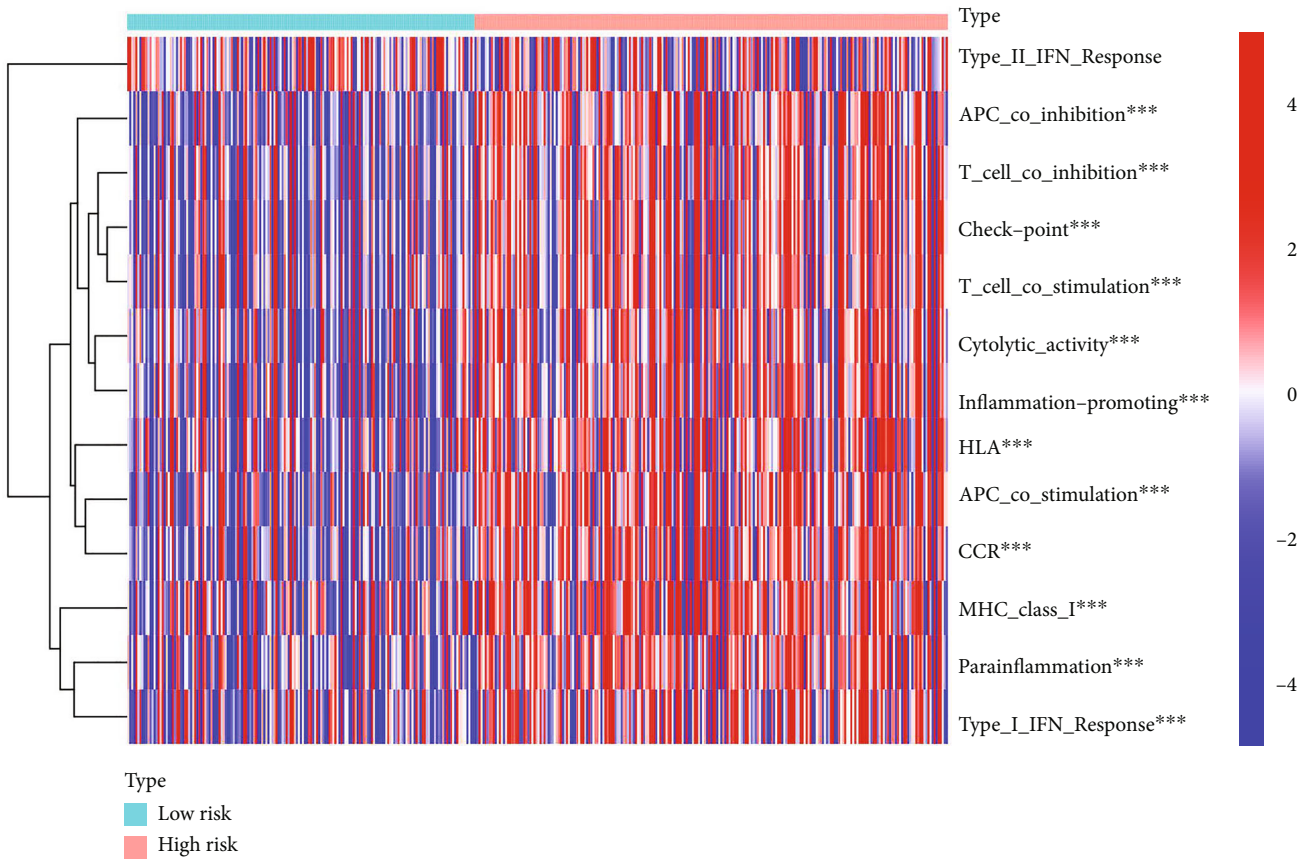

Figure 11: Immune-related function analysis of risk lncRNA.

Table 5: TMB of BLCA (partial examples).

ID	TMB
TCGA-DK-A6AW	86.52631579
TCGA-MV-A51V	33.47368421
TCGA-YC-A89H	32.84210526
TCGA-DK-A1AC	30.36842105
TCGA-DK-A3WW	25.55263158
TCGA-SY-A9G5	21.23684211
TCGA-XF-AAMG	20.60526316
TCGA-K4-A54R	19.86842105
TCGA-FD-A6TC	19.78947368
TCGA-E7-A7XN	19.34210526

analyzed using the R-Studio software (screening conditions: $P < 0.001$). From the IC50 values of drugs in the high-risk and low-risk groups, it could be found that bryostatin 1, doxorubicin, epothilone B, cyclopamine, dasatinib, FMK (Fluoromethyl Ketone), Genentech Cpd 10, obatoclax mesylate, paclitaxel, rapamycin, ruxolitinib, parthenolide, pazopanib, saracatinib, STF-62247, and other drugs indicated significant differences between the high- and low-risk groups, were more sensitive to the high-risk group, and could be found according to the correlation, IC50 value concentration of the drug, and negatively correlated with the risk score, the higher risk score, IC50 value concentration decreases (Figure 14).

4. Discussion

BLCA is one of the most common cancers in the urinary system. Although the diagnosis and treatment of BLCA have definite curative effects in the clinic, the disease may recur even after surgery. Therefore, screening of new BLCA biomarkers in the high-risk group is urgently needed for early and individualized treatment of patients with BLCA using potential drugs to improve the survival rate of patients. Cuproptosis is copper-dependent programmed cell death. The progress in human genome sequencing data indicated that lncRNAs play an indispensable role in the diagnosis, treatment, and prognosis of tumors [8–10]. Recent studies have shown that lncRNAs are involved in the occurrence and development of BLCA [11–13]. BLCA has been found to be associated with ferroptosis [14]. However, only a few studies on cuproptosis-related genes have been conducted. Therefore, it was of significant help to establish a prediction model of cuproptosis-related lncRNA based on the TCGA database to predict the prognosis of patients with BLCA and find new biomarkers for individualized treatment of high-risk patients.

In this study, 11 lncRNAs with independent prognostic significance were screened using univariate Cox regression analysis, Lasso regression analysis, and multivariate Cox

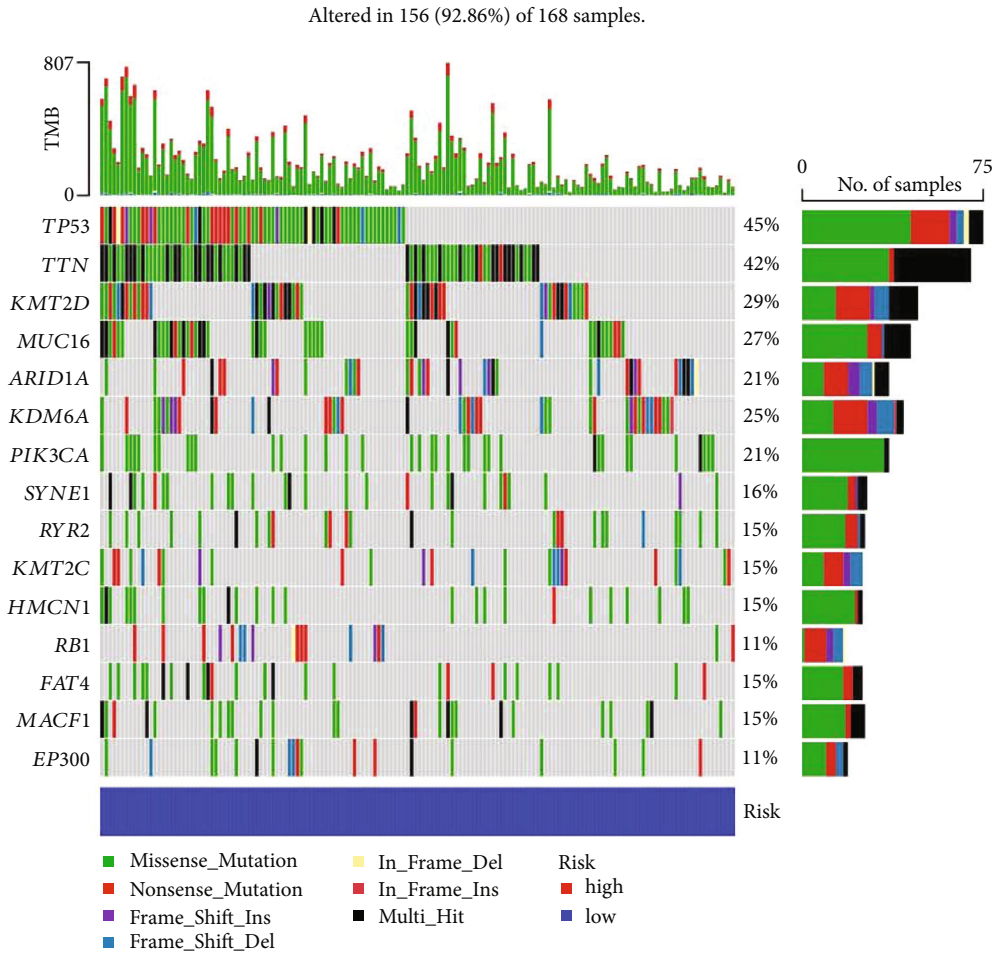

(a)

Figure 12: Continued.

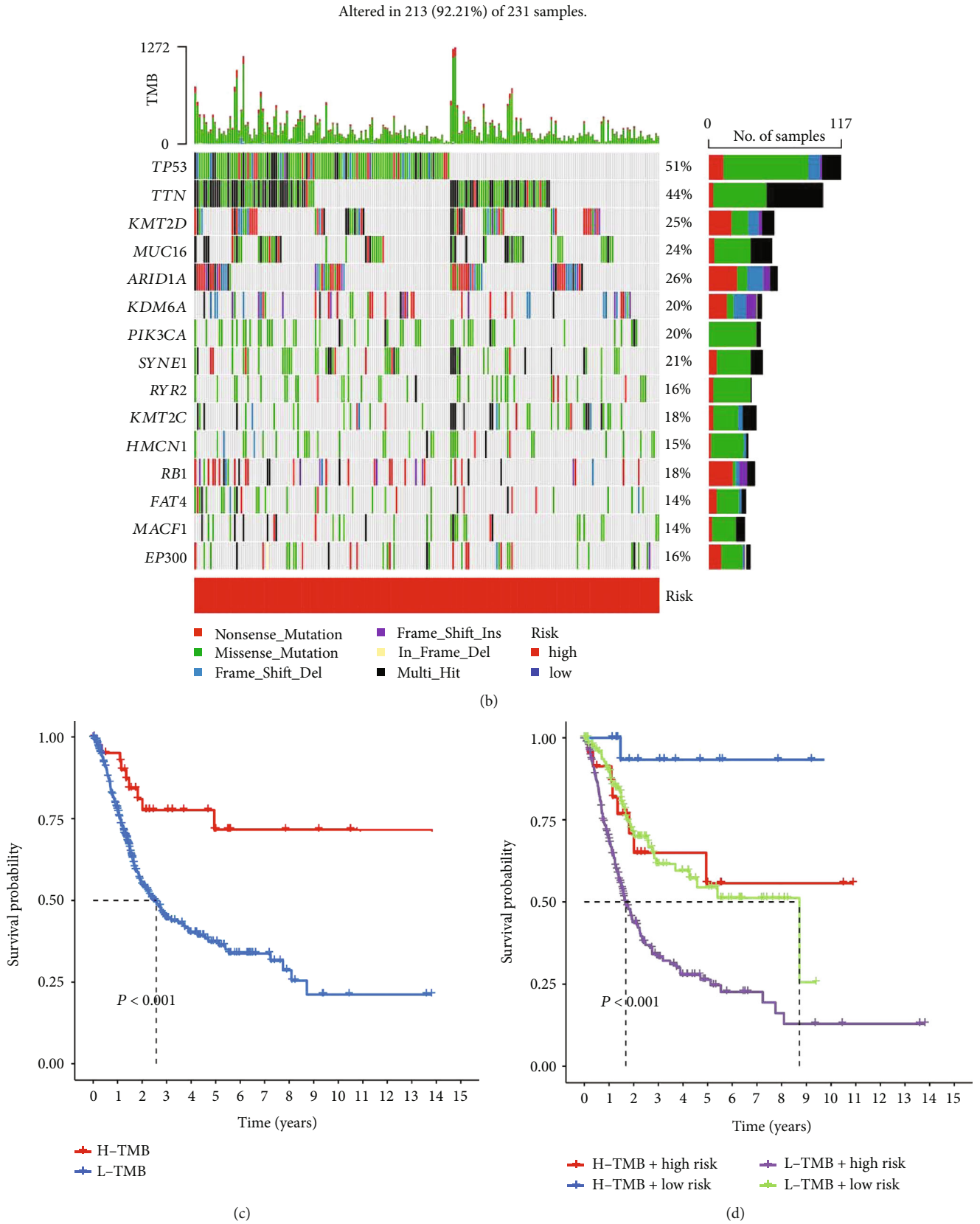

Figure 12: (a) Survival analysis of mutation frequency and mutation load of risk lncRNA. (b) Mutation frequency of high-risk lncRNA in high- and low-risk groups. (c) Survival analysis of TMB. (d) Survival analysis of high and low risk in TMB.

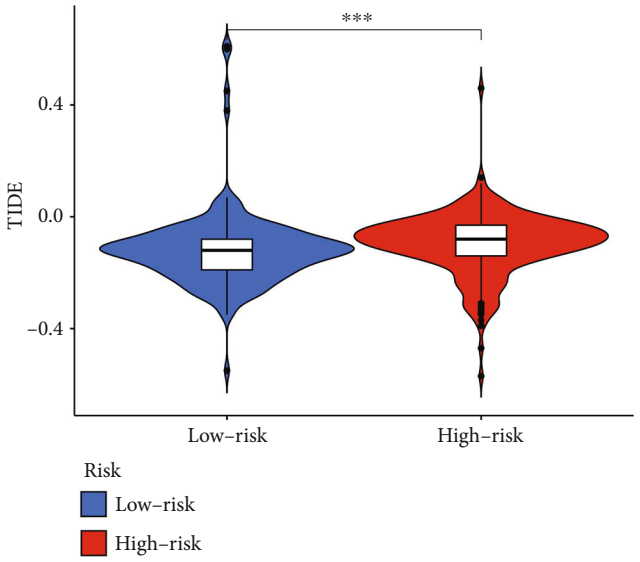

Figure 13: Analysis of immune evasion and immunotherapy in BLCA.

regression analysis to construct a prognostic model. Previous studies have shown that CASC20 is involved in the carcinogenesis of gastric cancer by competitively binding with Mir-143-5p and regulating the MEMO1 expression, thereby inducing epithelial–mesenchymal transition [15]. The SCAMP1 is a protein-coding gene. Among its related pathways is an innate immune system that plays an important role in the occurrence and development of ovarian cancer and glioma [16, 17]. SCAMP1-AS1 could inhibit the proliferation and migration of esophageal cancer TE-13 cells by targeting miR-483-5p, and SCAMP1-AS1 was downregulated in esophageal cancer cells [18]. Studies have shown that AC078778.1 is associated with the occurrence and development of BLCA [19]. NR2F2 antisense RNA 1 (NR2F2-AS1) expression is associated with renal clear cell carcinoma, gastric cancer, thyroid cancer, and other diseases. In thyroid cancer, NR2F2-AS1 promotes the proliferation and migration of thyroid cancer cells and inhibits cell death by regulating the miRNA-338-3p/CCND1 axis [20–22]. Studies have shown that downregulation of lncRNA MIR181A2HG (MIR181A2 host gene) by high glucose impairs vascular endothelial cell proliferation and migration through the dysregulation of the miRNAs/Akt2 axis [23]. At present, the remaining six lncRNAs (AC108066.2, AC110611.1, AC022165.1, AC010132.4, AC124283.3, and AP000593.3) associated with cuproptosis have not been reported in tumors; hence, further studies are needed to explore their significance. The BLCA prognostic model constructed based on 11 cuproptosis-related lncRNAs showed that the OS and PFS in the low-risk group were significantly better than those in the high-risk group in the survival analysis of the BLCA samples in the TCGA database. The survival status and risk score diagram revealed that the number of patients who died and the risk score continuously increased with the increase in the risk value. The analysis of the ROC curve and calibration chart indicated that the model had high sensitivity and accuracy in predicting the prognosis of BLCA, which could provide a potential direction for clinical research.

Most of the pathways were found to be correlated with immunity via enrichment analysis and immune-related function analysis of differentially expressed risk genes, and significant differences were observed in the immune-related functions. As parainflammation characterizing 50% of major cancer types has been shown to be correlated with p53 mutations and defective p53 pathways, parainflammation may serve as a driver of p53 mutagenesis and help in cancer prevention when treated with non-steroidal anti-inflammatory drugs [24, 25]. APC_co_stimulation, MHC_class_I, APC_co_inhibition, HLA, and Type_I_IFN_Reponse were significantly different among the BLCA subtypes. The study of the intratumoral immune microenvironment may provide a new perspective for BLCA treatment [26, 27]. Some studies found that T-cell co-stimulation in combination with targeting Focal adhesion kinase (FAK) drives enhanced anti-tumor immunity [28]. At present, no conclusive evidence suggests that cuproptosis is directly correlated with the occurrence of BLCA. However, this study will help explore the mechanism of cuproptosis-related lncRNAs.

Tumor mutational burden (TMB) was defined as the total number of detected somatic gene coding errors, base substitutions, and gene insertions or deletions per megabase [29]. PD-1 or its ligand (PD-L1) has achieved remarkable clinical efficacy in treating a variety of tumors. TMB, the newest marker for evaluating the efficacy of PD-1 antibodies, has been demonstrated in treating colorectal cancer with a deficiency in mismatch repair [30, 31]. The TMB level in tumor tissue can predict the efficacy of targeted therapy in patients with advanced non-small-cell lung cancer with driver mutations [32]. This study indicated that TMB could be considered an independent prognostic factor in BLCA.

Collectively, our results suggest that the proposed model, particularly the identified lncRNAs, could be promising biomarkers for estimating the prognosis of BC patients and could help clinicians to stratify patients into high- and low-risk groups, which could lead to more personalized treatment strategies. Furthermore, these lncRNAs could be investigated as therapeutic targets, as more in-depth understanding on their functional roles in BC and their involvement in cuproptosis could lead to the development of novel therapeutic approaches targeting these molecules or their downstream effectors. Thus, further research could explore the relationship between cuproptosis, lncRNAs, and BC in more detail, including studies on their underlying molecular mechanisms. Additionally, the proposed prognostic model could be validated using additional independent datasets, which would strengthen its potential use in clinical practice.

In conclusion, this study successfully constructed a prognostic model based on 11 promising lncRNAs with independent prognostic significance for patients with BC. The model effectively discriminated between high- and low-risk groups and demonstrated a strong association with immunity. Moreover, we identified potential treatment drugs with high sensitivity based on IC50 values, which provide important references for the potential development of personalized treatment strategies for BLCA patients.

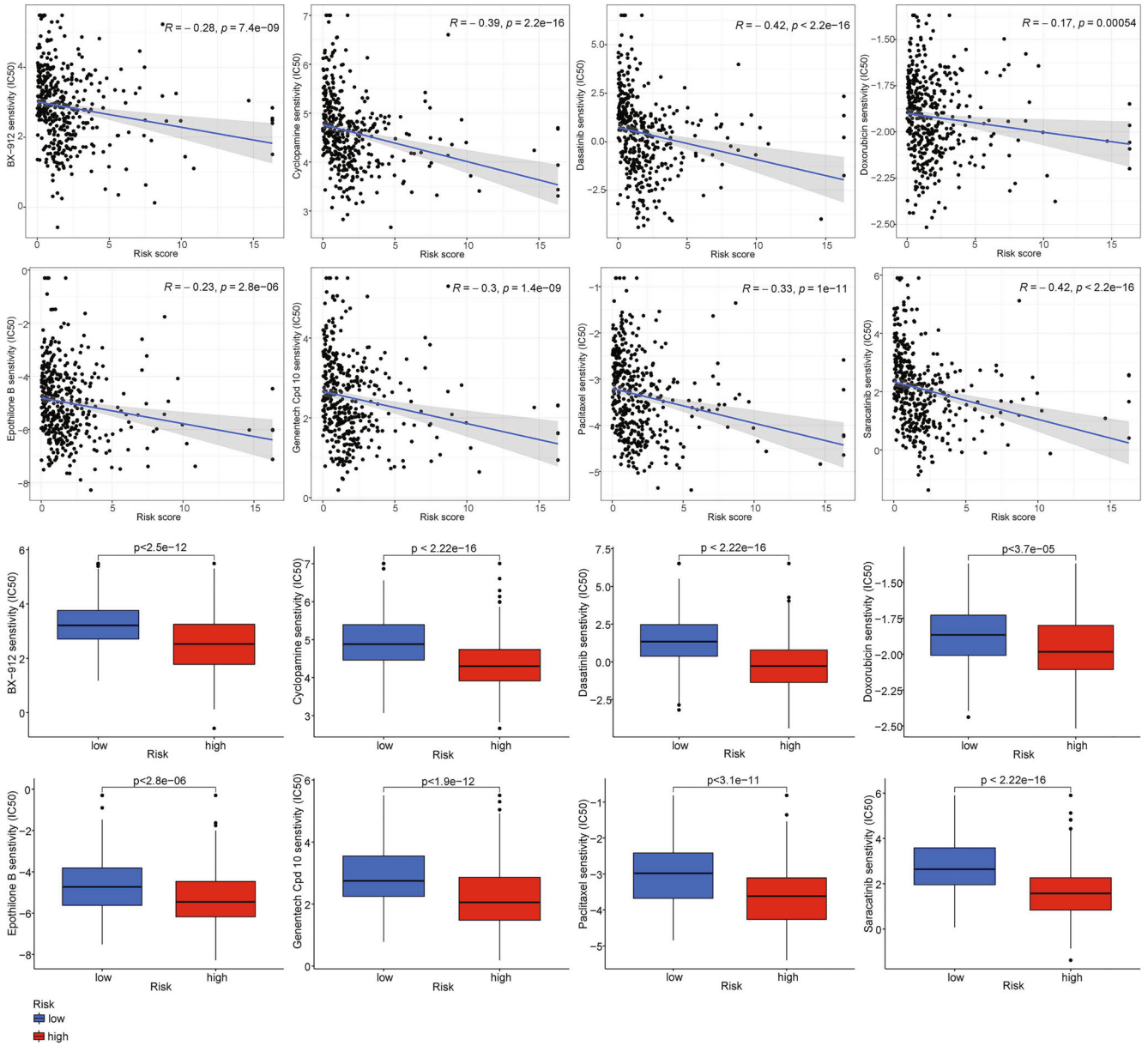

Figure 14: Screening of potential drugs for BLCA (partial examples).

Data Availability

Transcriptome expression data, clinical data, and mutation load data related to BLCA were downloaded from TCGA database (https://portal.gdc.cancer.gov). The transcriptome data uploaded to TIDE database (http://tide.dfci.harvard.edu/).

Conflicts of Interest

The author(s) declare(s) that they have no conflicts of interest.

Acknowledgments

We would like to thank TCGA database and TIDE database for providing high-quality data on BLCA. This work was supported by the National Natural Science Foundation of China (81800668) and Natural Science Foundation of Shanxi Province (201801D221276).

Supplementary Materials

Supplementary Materials. SupplementaryTable S1: The specific data description of Figure 1(a).

Supplementary Materials. SupplementaryTable S2: All data obtained after GO enrichment analysis of differential risk genes.

Supplementary Materials. SupplementaryTable S3: All data obtained after KEGG enrichment analysis of differential risk genes.

References

[1] J. Bellmunt, A. Orsola, J. J. Leow, T. Wiegel, M. de Santis, and A. Horwich, "Bladder cancer: ESMO practice guidelines for diagnosis, treatment and follow-up," *Annals of Oncology*, vol. 25, pp. iii40–iii48, 2014.

[2] L. A. Torre, F. Bray, R. L. Siegel, J. Ferlay, J. Lortet-Tieulent, and A. Jemal, "Global cancer statistics, 2012," *CA: A Cancer Journal for Clinicians*, vol. 65, no. 2, pp. 87–108, 2015.

[3] H. R. He, L. Li, A. Z. Feng et al., "The incidence and mortality of global bladder cancer from 1990 to 2017," *Chinese Journal of Evidence-Based Medicine*, vol. 20, pp. 1257–1265, 2020.

[4] C. J. Welty, T. H. Sanford, J. L. Wright et al., "The cancer of the bladder risk assessment (COBRA) score: estimating mortality after radical cystectomy," *Cancer*, vol. 123, no. 23, pp. 4574–4582, 2017.

[5] J. Li, Y. D. Liu, and L. Q. Beng, "Clinical effect and prognosis of partial bladder resection combined with radiotherapy and chemotherapy in patients with muscle invasive bladder cancer," *Journal of Clinical Urology*, vol. 32, pp. 767–770, 2017.

[6] W. He and J. Hang, "The update interpretation of 2020 EAU bladder cancer guideline (part I)—progress of muscle-invasive and metastatic bladder cancer," *Chinese Journal of Urology*, vol. 41, pp. 492–493, 2020.

[7] P. Tsvetkov, S. Coy, B. Petrova et al., "Copper induces cell death by targeting lipoylated TCA cycle proteins," *Science*, vol. 375, no. 6586, pp. 1254–1261, 2022.

[8] S. Fattahi, N. Nikbakhsh, H. Taheri, E. Ghadami, M. Ranaee, and H. Akhavan-Niaki, "LINC02688 and PP7080 as novel biomarkers in early diagnosis of gastric cancer," *Non-Coding RNA Research*, vol. 6, no. 2, pp. 86–91, 2021.

[9] Y. Q. Zhao, G. L. Liu, H. C. Wang et al., "Influence of LncRNA NKILA on biological behavior of malignant tumors and related mechanism," *Cancer Research on Prevention and Treatment*, vol. 49, pp. 67–71, 2022.

[10] W. Q. Liu, Y. Cao, B. Cheng et al., "The mechanism and research progress of lncRNA as potential antitumor drug targets," *Northwest Pharmaceutical Journal*, vol. 2, pp. 215–219, 2014.

[11] Z. S. Chen, B. Ni, L. Shu et al., "LncRNA H19 promotes bladder cancer by downregulating PTEN via DNMT1," *Chinese Journal of Surgical Oncology*, vol. 14, pp. 138–144, 2022.

[12] A. Rakhshan, M. H. Esmaeili, M. S. Kahaei et al., "A single nucleotide polymorphism in GAS5 lncRNA is associated with risk of bladder cancer in Iranian population," *Journal of International Management*, vol. 26, pp. 1251–1254, 2020.

[13] R. R. Xia, P. Y. Liang, S. X. Wang et al., "Effect of lncRNA HOXA11-AS on proliferation, migration and invasion of bladder urothelial carcinoma cell and its mechanism abstract," *Chinese Journal of Immunology*, vol. 37, pp. 51–56, 2021.

[14] M. X. Ma, F. C. Zhang, H. G. Ma et al., "Construction and analysis of a prognostic model of bladder cancer based on ferroptosis-related lncRNA," *Journal of Modern Urology*, vol. 27, pp. 253–260, 2022.

[15] K. S. Shan, W. W. Li, W. Ren et al., "LncRNA cancer susceptibility 20 regulates the metastasis of human gastric cancer cells via the miR-143-5p/MEMO1 molecular axis," *World Journal of Gastroenterology*, vol. 28, no. 16, pp. 1656–1670, 2022.

[16] R. Song, Z. H. Liu, L. J. Lu, F. Liu, and B. Zhang, "Long non-coding RNA SCAMP1 targets miR-137/CXCL12 Axis to boost cell invasion and angiogenesis in ovarian cancer," *DNA and Cell Biology*, vol. 39, no. 6, pp. 1041–1050, 2020.

[17] Z. Q. Zong, Y. C. Song, Y. X. Xue et al., "Knockdown of LncRNA SCAMP1 suppressed malignant biological behaviours of glioma cells via modulating miR-499a-5p/LMX1A/NLRC5 pathway," *Journal of Cellular and Molecular Medicine*, vol. 23, no. 8, pp. 5048–5062, 2019.

[18] A. R. Zheng, L. Lei, X. J. Teng et al., "The effect of long-chain noncoding RNA SCAMP1-AS1 on the proliferation and migration of esophageal cancer cells by targeting and regulating miR-483-5p," *Chinese Journal of Postgraduates of Medicine*, vol. 45, pp. 487–492, 2022.

[19] J. W. Wang, C. Y. Zhang, Y. Wu, W. He, and X. Gou, "Identification and analysis of long non-coding RNA related miRNA sponge regulatory network in bladder urothelial carcinoma," *Cancer Cell International*, vol. 19, no. 1, p. 327, 2019.

[20] L. Chen, D. X. Zhang, T. Ding et al., "LncRNA NR2F2-AS1 upregulates Rac1 to increase cancer stemness in clear cell renal cell carcinoma," *Cancer Biotherapy and Radiopharmaceuticals*, vol. 35, no. 4, pp. 301–306, 2020.

[21] W. W. Zuo, C. L. Li, and F. Pan, "Effect of long non-coding RNA NR2F2-AS1 on proliferation and apoptosis of gastric cancer cells," *Journal of Modern Oncology*, vol. 29, pp. 739–743, 2021.

[22] F. Guo, Q. F. Fu, Y. Wang, and G. Sui, "Long non-coding RNA NR2F1-AS1 promoted proliferation and migration yet suppressed apoptosis of thyroid cancer cells through regulating miRNA-338-3p/CCND1 axis," *Journal of Cellular and Molecular Medicine*, vol. 23, no. 9, pp. 5907–5919, 2019.

[23] S. H. Wang, B. Zheng, H. Y. Zhao, Y. Li, X. Zhang, and J. Wen, "Downregulation of lncRNA MIR181A2HG by high glucose impairs vascular endothelial cell proliferation and migration through the dysregulation of the miRNAs/AKT2 axis," *International Journal of Molecular Medicine*, vol. 47, no. 4, p. 35, 2021.

[24] A. Lasry, D. Aran, A. Zinger et al., "S-6: parainflammation in cancer," *Cytokine*, vol. 70, no. 1, p. 22, 2014.

[25] D. Aran, A. Lasry, A. Zinger et al., "Widespread parainflammation in human cancer," *Genome Biology*, vol. 17, no. 1, p. 145, 2016.

[26] Q. Z. Luo and T. A. Vögeli, "A methylation-based reclassification of bladder cancer based on immune cell genes," *Cancers*, vol. 12, no. 10, p. 3054, 2020.

[27] J. M. Romero, B. Grunwald, G. H. Jang et al., "A methylation-based reclassification of bladder cancer based on immune cell genes," *Clinical Cancer Research*, vol. 26, no. 8, pp. 1997–2010, 2020.

[28] M. Canel, D. Taggart, A. H. Sims, D. W. Lonergan, I. C. Waizenegger, and A. Serrels, "T-cell co-stimulation in combination with targeting FAK drives enhanced anti-tumor immunity," *eLife*, vol. 9, article e48092, 2020.

[29] M. Yarchoan, A. Hopkins, and E. M. Jaffee, "Tumor mutational burden and response rate to PD-1 inhibition," *The New England Journal of Medicine*, vol. 377, no. 25, pp. 2500–2501, 2017.

[30] D. T. Le, J. N. Durham, K. N. Smith et al., "Mismatch-repair deficiency predicts response of solid tumors to PD-1 blockade," *Science*, vol. 357, no. 6349, pp. 409–413, 2017.

[31] D. T. Le, J. N. Uram, H. Wang et al., "PD-1 blockade in tumors with mismatch-repair deficiency," *The New England Journal of Medicine*, vol. 372, no. 26, pp. 2509–2520, 2015.

[32] L. Tong, N. Ding, J. M. Li et al., "Relationship between tumor mutational burden and efficacy of targeted therapies in patients with advanced non-small cell lung cancer," *Chinese Journal of Clinical Medicine*, vol. 26, pp. 538–542, 2019.